Elastic Moduli of Asymmetric Ultrathin Free-Standing Polyelectrolyte Nanocomposites

James K. Ferri,*,†,‡ Wen-Fei Dong,‡ Reinhard Miller,‡ and Helmuth Möhwald‡

Department of Chemical Engineering, Lafayette College, Easton, Pennsylvania 18042, and Max Planck Institute of Colloids and Interfaces, Golm/Potsdam, D-14476, Germany

Received July 26, 2005; Revised Manuscript Received December 20, 2005

ABSTRACT: We have developed a novel technique for the elucidation of the mechanical behavior of ultrathin free-standing materials and demonstrate results using polyelectrolyte nanocomposites with thicknesses between 1 and 10 nm. In short, a charged molecular template is deposited on a pendant drop and compressed to present a defined surface charge density to the subphase of the drop. The subphase is then cycled alternately between polyelectrolyte solutions to achieve electrostatic layer-by-layer assembly of an ultrathin nanocomposite at the drop surface. The stress response of the membrane-laden drop to dilation of its surface as measured by axisymmetric drop shape analysis is compared with a two-dimensional continuum model. The impact of surface charge density of the template and the film thickness on the two-dimensional elastic modulus, E_s, of the nanocomposite were assessed, and mechanical behavior consistent with that of an elastomeric solid is demonstrated.

Introduction

The realization of devices with nanometer scale elements hinges on the ability of low-dimensional materials to sustain mechanical loads during fabrication, assembly, and use. Although investigations describing new routes to produce nanomaterials with unique chemical functionality and transport properties have been reported, detailed studies of the mechanical properties of these materials[1−3] are relatively scarce because quantitative experimental techniques are limited due to the length scales involved.

Ultrathin free-standing films have recently received increasing attention due to their potential use as micromechanical sensors,[4] actuators,[5] and barrier materials.[6] An increasing number of experimental results have shown that thin films exhibit dramatically different behavior as compared to bulk materials, i.e., transport,[7,8] glass transition,[9−11] and stress to failure,[12] although the mechanisms responsible for these phenomena are still not fully understood. For experimental investigations into these, a prerequisite is the fabrication of truly free-standing thin films. The layer-by-layer technique (Lbl) for preparing multilayer films is attractive, because it allows tunable composition and functionality, versatile and aqueous-based preparation procedures on substrates of arbitrary shape, and accurate thickness control with nanometer precision.[13,14] Normally, free-standing polyelectrolyte thin films (PEMs) are created via the alternating deposition of oppositely charged polyelectrolytes (or other ionic species) onto solid templates modified with degradable precursor layers, viz. a pH-sensitive, sacrificial layer[15] or template,[16−18] followed by template removal. Successful investigations have focused on the mechanical properties of polyelectrolyte (PE) multilayers, PE/metal composite[19] or PE/carbon nanotube composite[15] (CNT) films, and PE capsules.[17,18]

However, in each of these cases, film preparation relies strongly on the solid substrate and template removal process. For example, sacrificial layers of cellulose acetate are precoated on solid substrate for preparation of PE/metal[12] or PE/CNT[15] films, and polyelectrolyte capsules are made by melamine formaldehyde microparticles (acid-soluble), polystyrene (solvent-soluble), carbonate particles (acid- or EDTA-soluble) or SiO_2 particles (HF-soluble), etc.[16,18,20] Although these PEMs ultimately become free-standing films after template removal, artifacts of the assembly process carried out on an immobile surface remain. Additionally, template residue and solvent effects from the removal process on the nanocomposite structure can influence experimental characterization. Perhaps most importantly, mechanical characterization of any kind of ultrathin free-standing polymeric film with a thickness below 10 nm has not yet been reported.[20]

In this article, we report a new technique for the mechanical characterization of free-standing ultrathin nanocomposite films on a pendant drop using Lbl adsorption of polyelectrolytes onto a charged insoluble monolayer template pinned to the aqueous/air interface. The geometry of the drop interface admits dilational deformation of the resultant membrane otherwise not possible on a planar interface. Because the aspect ratio of the nanocomposite (thickness to width) is smaller than 10^{-6}, a large scale ensemble average of the mechanical properties of a free-standing film, inaccessible by other methods, is achieved. The elastic moduli of these membranes is measured by a novel pendant drop technique. The moduli measured for these materials are consistent with a rubbery polymeric material. Therefore, it is likely that the nanocomposites in this study are likely to be elastomeric structures. This is verified by demonstration that they stretch semireversibly upon large deformation with an increasing dependence of the film surface elastic modulus on film thickness and template charge density.

Experimental Section

A schematic of the technique for the synthesis of an ultrathin free-standing nanocomposite is shown in Scheme 1. A dimyristoylphosphatidyl glycerol (DMPG) anionic lipid monolayer is deposited onto a pendant drop of aqueous saline solution and compressed to achieve a specified surface density of template molecules. The subphase of the drop is then exchanged maintaining constant surface area with a subphase containing poly(allylamine hydrochloride) (PAH). Alternate cycles of PAH and poly sodium 4-styrenesulfonate (PSS) and intermittent flushing with polyelec-

* To whom correspondence should be addressed: ferrij@lafayette.edu.
† Lafayette College.
‡ Max Planck Institute of Colloids and Interfaces.

10.1021/ma0516485 CCC: $33.50
Published on Web 01/27/2006

Scheme 1. Preparation of Ultrathin Freestanding Polyelectrolyte Nanocomposites[a]

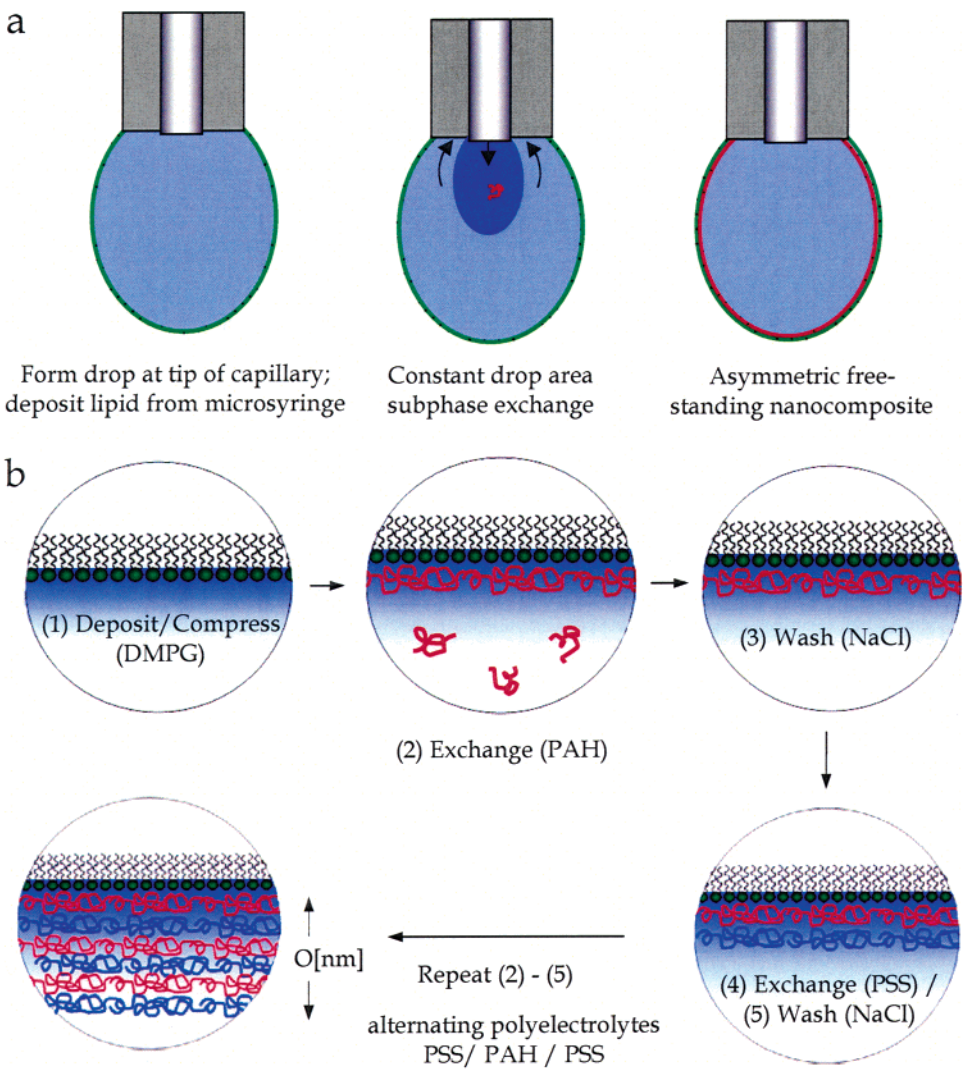

[a] Key: (a) polylelectrolyte adsorption onto a lipid monolayer by subphase exchange in a pendant drop; (b) schematic of the multilayer assembly process at the air−water interface.

trolyte-free saline solution result in free-standing polymeric nanocomposites having a thickness which is defined by the number of adsorption layers.[21]

Dimyristoylphosphatidyl glycerol (DMPG), poly(sodium 4-styrenesulfonate) sodium salt (PSS, $M_w \sim 70$ kDa), poly(allylamine hydrochloride) (PAH, $M_w \sim 70$ kDa) were all purchased from Aldrich and used as received except for PSS, which was dialyzed before use (M_w 50 kDa cut off). Lipid spreading solution was prepared using ultrapure chloroform and methanol, approximately (3:1 v:v) from J. T. Baker. The water in all experiments was purified in a three-stage Milli-Q Plus 185 purification system and had a resistivity higher than 18.2 MΩ/cm. The experimental setup is a pendant drop tensiometer (PAT1 from Sinterface Technologies, Germany) equipped with a coaxial capillary dosing system. In short, a silhouette of a pendant drop formed at the tip of a capillary is cast onto a CCD camera. The drop shape is digitized and recorded over time to fit to the Young−Laplace equation to accurately (± 0.1 mN/m) determine isotropic surface stress and control the drop interfacial area by feedback control of the digititized image and flow rate from the primary syringe. The drop subphase is exchanged at constant surface area by injection and withdrawal of fluid through concentric capillaries on which the drop was formed. Further details of the technique for preparation of ultrathin free-standing nanocomposites are described in detail in recent publications.[22−24] Nanocomposites of DMPG−(PAH/PSS)$_n$ were prepared as described above at a constant drop area ($A = 25$ mm^2).

The mechanical behavior of the free-standing films was investigated by dilation of the drop area and measurement of the isotropic surface stress response by axisymmetric drop shape analysis. The drop interfacial area (A) was dilated from $A_0 = 25$ to $A = 40$ mm^2 at a rate of 0.15 mm^2 s^{-1} by injecting liquid into the drop subphase from the capillary via the syringe pump, holding it for 300 s, and contracting it to the original size at the same rate by withdrawal of liquid from the drop. The resulting isotropic surface stress-interfacial area curves were used to calculate the elastic properties of the nanocomposite as described below. Prior to the synthesis of each film, the stress−area curve of the molecular template was checked for consistency.

Theory

The thin film on the drop surface is assumed to be an elastic, homogeneous, isotropic membrane that is spatially constrained to the interface. The membrane is unstretched in the reference configuration with an initial uniform thickness of d, which is small with respect to the radii of curvature of the drop. Under these conditions, bending stresses are negligible. The deformation of the drop is assumed to be quasi-static and axisymmetric, where the principle stretches (λ_1, λ_2) are defined as the stretches in the meridonal (1) and azimuthal (2) directions, i.e. $\lambda_1 = \partial\xi(z_0)/\partial\xi_0(z_0)$ and $\lambda_2 = r(z_0)/r_0(z_0)$, and the product $\lambda_1\lambda_2$ is equal to the ratio of the area in the deformed configuration with respect

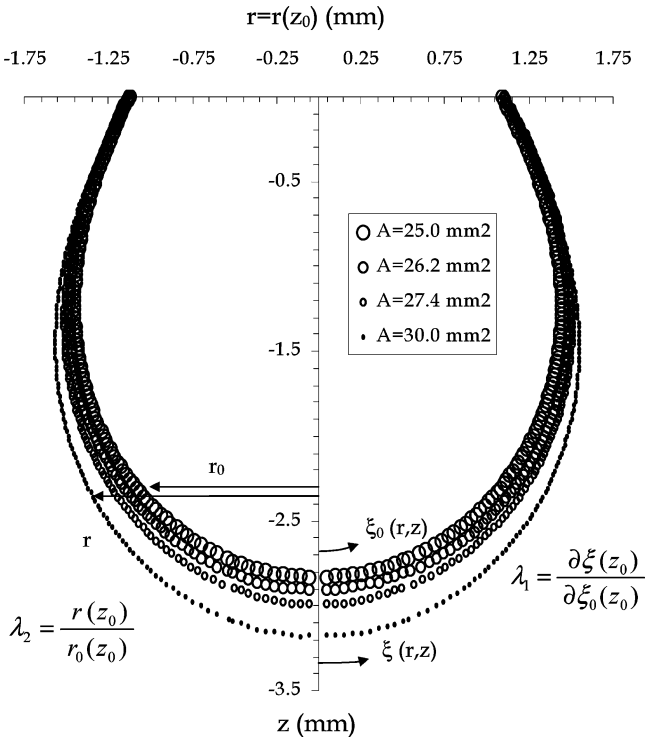

Figure 1. Observation of dilational deformation of a single pendant drop encapsulated by a DMPG−(PAH/PSS)$_{n=3}$ nanocomposite membrane.

to the unstretched state, i.e., A/A_0. The coordinate system for the deformation and experimental observations of drop deformation from a typical experiment are shown in Figure 1.

The tangential component of the momentum balance in the meridonal direction is given by

$$\frac{\partial \tau_1}{\partial s} - \frac{1}{r}\frac{\partial r}{\partial s}(\tau_2 - \tau_1) = 0 \tag{1}$$

and the normal component of the momentum balance is

$$\kappa_1 \tau_1 + \kappa_2 \tau_2 = \Delta P \tag{2}$$

where the interfacial curvature is defined in the usual way; i.e., $\kappa_1 = -(r''/\sqrt{1-r'})$ and $\kappa_2 = (1/r)\sqrt{1-r'^2}$.

Evans and Skalak[25] proposed a constitutive law for a homogeneous, isotropic two-dimensional elastic material, namely

$$\tau_1 = K_S(\lambda_1\lambda_2 - 1) + \mu_S\frac{\lambda_1^{\,2} - \lambda_2^{\,2}}{2\lambda_1^{\,2}\lambda_2^{\,2}} \tag{3}$$

where (τ_2) is defined by switching index 1 to 2.

If the membrane deformation is isotropic; i.e., $\lambda_1 \approx \lambda_2$, the stress response is also isotropic and can be defined by the average of the two principle stresses:

$$\gamma = 1/(2(\tau_1 + \tau_2)) \tag{4}$$

There are two consequences. First, the momentum balance, i.e., eqs 1 and 2 reduce to the Young−Laplace equation, which relates the pressure jump across an interface to its curvature and isotropic or surface tension. Second, the constitutive eq 3 can be reduced to show that γ is linearly dependent on the strain invariant, $\alpha = \lambda_1\lambda_2 - 1$, or the area dilation of the membrane. In the limit of small deformation,[26] the area dilational modulus of the membrane, K_S, is related to the surface Young's modulus, E_S, and Poisson ratio, ν_S, by

$$K_s = \frac{E_s}{2(1-\nu_s)} \tag{5}$$

Results and Discussion

Consider a freshly prepared ultrathin nanocomposite on the surface of a pendant drop. The initial drop shape is determined by the surface tension of the template-covered interface; i.e., there is an initial interfacial tension. However, the film is synthesized onto this shape, so the film has no internal stress; i.e., an initial stress-free state in the film, but the surface tension of the interface is nonzero.

As dilational deformation of the drop area proceeds and α increases, the membrane elasticity resists the deformation resulting in a surface stress (γ) that develops in an attempt to restore the drop to its undeformed state. (See for example, data shown in Figure 2.) By measuring the slope of the increase (K_s) in the limit of small deformation, the constitutive parameters of the membrane can be calculated using the relationship in (3).

The mechanical response of the surface stress to the deformation is determined by the microstructure of the membrane. In the case of an ultrathin polyelectrolyte nanocomposite, it might be expected that the density of electrostatic cross-links and film thickness both play a role. To investigate the impact of cross-link density on the mechanics of a free-standing polyelectrolyte nanocomposite, the use of a molecular monolayer as a template is attractive, because the charge density of the interface can be precisely controlled without changing its chemical composition. The lipid used in this study forms a stable monolayer with no surface phase transitions. For the phosphatidic acid group at pH 7 and high salt concentration, the degree of dissociation is greater than (90%) for surface densities between $40 < 1/\Gamma < 120$ Å^2/molecule.[27] Thus, the surface charge density of the template, σ_T, can be assumed a spatially uniform and linear function of surface density. It is well-known that the equation of state; i.e., the dilational modulus K_s as a function of surface density for a lipid monolayer, is nonlinear. The behavior of the template alone was investigated at charge densities of $\sigma_T = 0.57$, 0.61, and 0.65 nm^2/e. In the limit of small deformation ($\alpha < 0.05$), K_s was found to be 88, 82, and 70 mN/m, respectively. (Data are given in the Supporting Information.)

To calculate a surface elasticity, E_s, from the surface dilational modulus, K_s, a value of the surface Poisson ratio, ν_s, must be assumed. For two-dimensional solids, the Poisson ratio is constrained between $-1 < \nu_s < 1$. Pieper et al.[28] have reported values of the Poisson ratio for cross-linked interfacial polymeric adsorption layers to be zero or slightly negative. In a recent advance, conceptual laminate structures have been presented which give rise to negative Poisson's ratios combined with mechanical isotropy in two dimensions or in three dimensions. By appropriate choice of constituent properties laminae, one can achieve Poisson's ratios approaching the lower limit of -1.[29] However, the choice of Poisson ratio effects neither the magnitude nor the trends in elasticity for the present study. For $\nu_s = 0$, E_s was 177, 164, and 137 mN/m, respectively.

Figure 2 shows the isotropic surface stress γ as a function of the area dilation of the surface α for different values of surface template charge densities σ_T for the nanocomposites of varying thickness, i.e., DMPG−(PAH/PSS)$_{n=1-3}$. These are the interfacial stress−strain curves; the steepest slope of which in the limit of small deformation is used to calculate the surface Young's modulus, E_s. After the addition of one bilayer, i.e., *n*

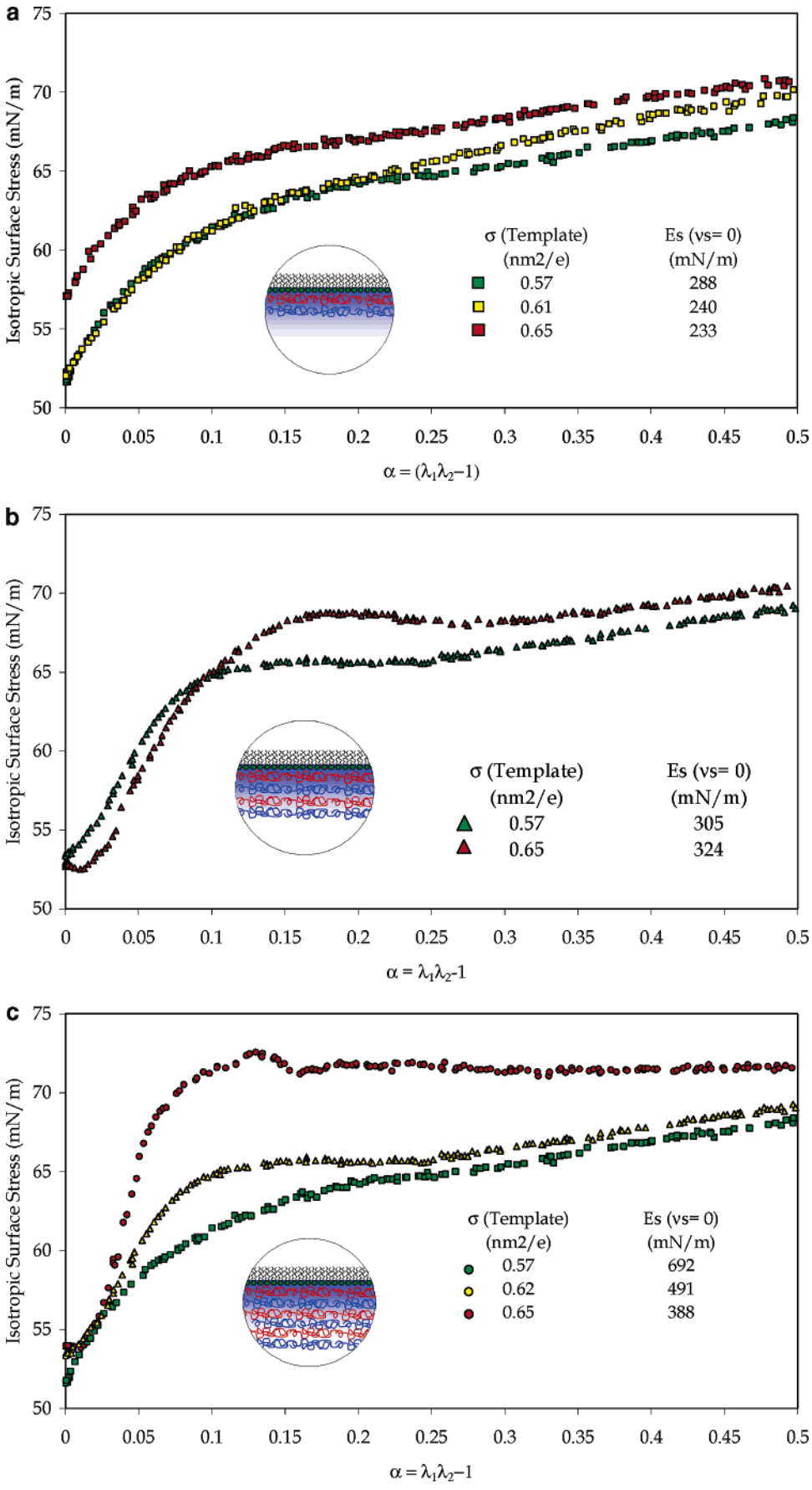

Figure 2. Dependence of isotropic surface stress γ on area dilation α for nanocomposites on templates of varying surface charge density for (a) DMPG−(PAH/PSS)$_{n=1}$, (b) DMPG−(PAH/PSS)$_{n=2}$, and (c) DMPG−(PAH/PSS)$_{n=3}$.

= 1, the E_s increases to 288, 240, and 233 mN/m; see data in Figure 2a. The largest increase in E_s occurs at the highest surface charge density of the template reflecting the influence of the template on the density of electrostatic cross-links in the

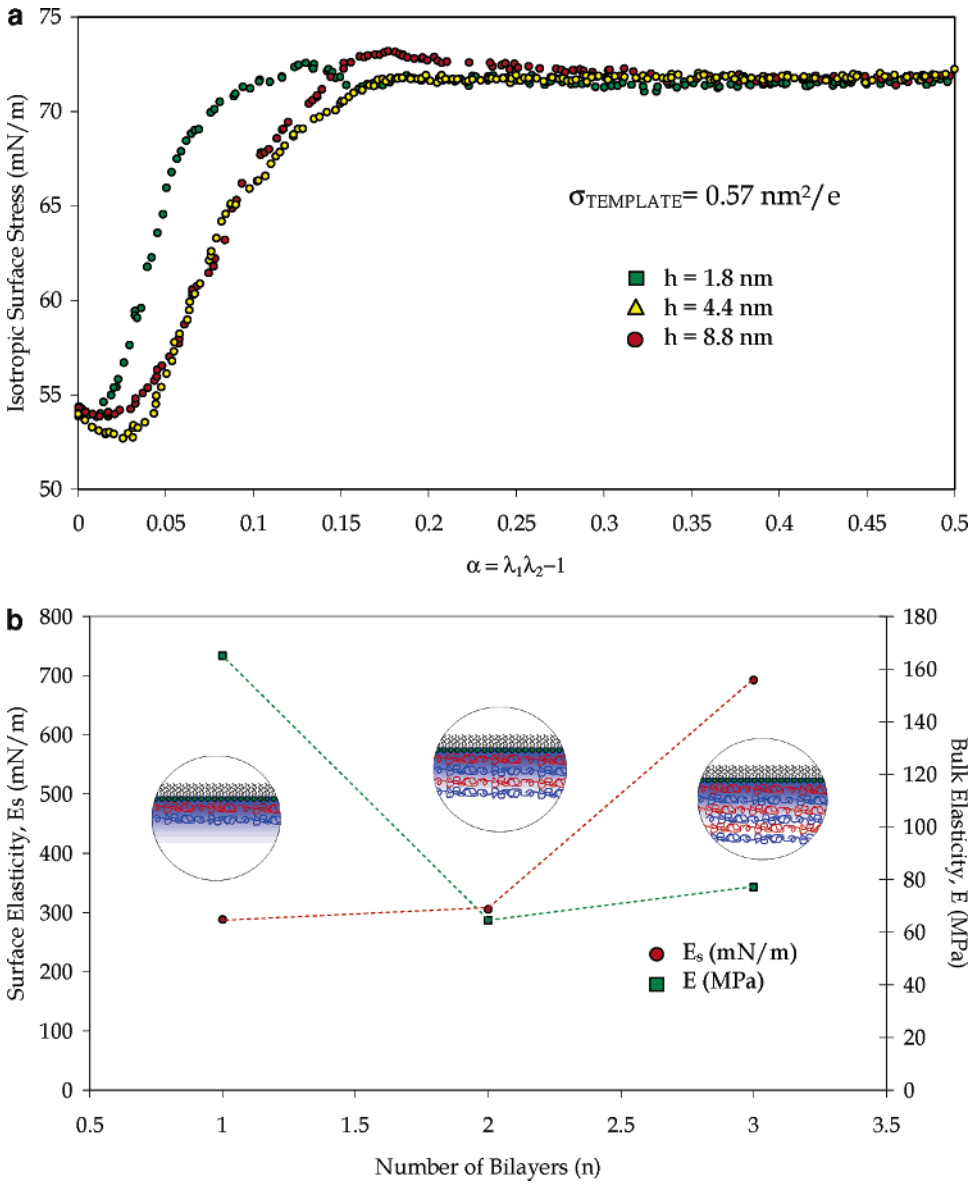

Figure 3. Influence of confinement on ultrathin membrane mechanics: (a) dependence of isotropic surface stress γ on area dilation α (σ_T =57 nm^2/e) DMPG−(PAH/PSS)$_{n=1-3}$ and (b) dependence of surface and bulk elastic moduli on number of bilayers (i.e., film thickness.)

polyelectrolyte network. Because the increase in E_s is not constant, the dependence of the film mechanics on σ_T is not likely to be an artifact of the stress response of the template alone. This is evident upon the addition of the second bilayer; although the surface modulus increases for both $\sigma_T = 0.57$ and 0.65 nm^2/e, the increase is larger for the film with the lower template density as shown in Figure 2b. Figure 3b shows the stress response for nanocomposites for three bilayers, i.e., $n = 3$. Again the influence of σ_T is evident, showing the maximum elasticity for the film synthesized on the template with the highest charge density. These results demonstrate that the nanocomposite's memory of the template register extends at least 10 nm into the film and underscores the impact of the substrate chemistry on the mechanical behavior, a systematic study of which to our knowledge has not yet been reported.

The thickness dependence of the mechanical properties of polymeric ultrathin films is also of significant interest, because the role of nanoconfinement in the dynamics of polymeric systems is not yet clear. For nanoscopically confined films, it has been demonstrated that the glass transition temperature decreases with film thickness because of the enhanced mobility of the polymer chains near a free surface. Therefore, one would expect that a film transition from glass to rubber would be accompanied by a corresponding change in the elastic modulus. Recently, Nolte[30] reported values of the Young's modulus of (PSS/PAH) multilayers in the dry state measured by stress-induced mechanical buckling instabilities and showed a decreasing dependence of the film elasticity on thickness. For a film thickness above 80 nm, the Young's modulus is constant at 4.4 GPa, which is consistent with behavior of a glassy polymer. However, the elastic modulus is clearly shown to decrease strongly for film thicknesses between 40 and 20 nm. This trend is consistent with a transition from a glassy to rubbery state as the degree of film confinement decreases; however, to the best of our knowledge, measurements of the elastic modulus for polymeric films between 1 and 10 nm have not been reported.

The influence of thickness on the mechanical behavior of the nanocomposites in this study prepared at ($\sigma_T = 57$ nm^2/e) is shown in Figure 3a. A dramatic increase in the surface elasticity is evident; as the film thickness increases from $n = 2$ to 3, the surface modulus increases from 305 to 692 mN/m. The bulk elastic modulus of the film can be found by normalizing the surface modulus by the film thickness, i.e., $E = E_s/d$. A previous study of the same multilayer nanocomposites

on a planar aqueous-air interface showed nonlinear film growth with the film thickness, $h = 2$, 5, and 9 nm for $n = 1$, 2, and 3.[21] Figure 3b shows the surface and corresponding bulk values of the Young's modulus as a function of thickness. Although the surface elastic modulus exhibits a dramatic increase as a function of film growth, the bulk elasticity (i.e., the Young's modulus) is approximately constant for films thicker than 5 nm ($n = 2$) and has a value of approximately 80 MPa which suggests that out of plane polyelectrolyte coupling is limited to about two layers. The magnitude of the elastic modulus is consistent with an elastomeric rubber. For such a material, some degree of a reversibility and viscoelastic response would be expected; both were experimentally observed. (See Supporting Information for data.)

Conclusions

In summary, we have presented a technique for the measurement of the mechanics of ultrathin free-standing films and results for the model system DMPG−(PAH/PSS)$_{n=1-3}$. These experiments represent the first mechanical measurements of polymeric free-standing materials confined between 1 and 10 nm. Although results for thicker films ($h > 20$ nm) display glassy mechanical behavior, these measured values of the Young's modulus in this study are consistent with an elastomeric rubber and suggest that a confinement dependence of the glass transition may also occur for nanocomposite polyelectrolyte ultrathin films.

Acknowledgment. J.K.F. is grateful for the support of the Alexander von Humboldt Foundation in the form of a research fellowship.

Supporting Information Available: Figure S1, isotropic surface stress γ vs area dilation α for template (DMPG) as a function of surface charge density, Figure S2, experimental profiles of isotropic surface stress γ and area A vs time for DMPG−(PAH/PSS)$_{n=1}$ and template (DMPG) as a function of template charge density, Figure S3, experimental profiles of isotropic surface stress γ and area A vs time for DMPG−(PAH/PSS)$_{n=2}$ and template (DMPG) as a function of template charge density, Figure S4, experimental profiles of isotropic surface stress γ and area A vs time for DMPG−(PAH/PSS)$_{n=3}$ and template (DMPG) as a function of template charge density, Figure S5, (semi-)reversibility of stress/area for DMPG−(PAH/PSS)$_{n=3}$, and Figure S6, stress relaxation after step strain in area for DMPG−(PAH/PSS)$_{n=2}$. This material is available free of charge via the Internet at http://pubs.acs.org.

References and Notes

(1) Haque, M. A.; Saif, M. T. A. *Proc. Natl. Acad. Sci. U.S.A.* **2004**, *101*, 6335−6340.
(2) Stafford, C. M.; Harrison, C.; Beers, K. L.; Karim, A.; Amis, E. J.; Vanlandingham, M. R.; Kim, H. C.; Volksen, W.; Miller, R. D.; Simonyi, E. E. *Nat. Mater.* **2004**, *3*, 545−550.
(3) Herminghaus, S.; Jacobs, K.; Seemann, R. *Eur. Phys. J. E* **2001**, *5*, 531−538.
(4) Jiang, C. Y.; Markutsya, S.; Pikus, Y.; Tsukruk, V. V. *Nat. Mater.* **2004**, *3*, 721−728.
(5) Rubner, M. *Abstr. Pap. Am. Chem. Soc.* **2003**, *225*, U616−U616.
(6) Nolte, M.; Schoeler, B.; Peyratout, C. S.; Kurth, D. G.; Fery, A. *Adv. Mater.* **2005**, *17*, 1665−1669.
(7) Huang, Y.; Paul, D. R. *Polymer* **2004**, *45*, 8377−8393.
(8) Huang, Y.; Paul, D. R. *J. Membr. Sci.* **2004**, *244* (1−2), 167−178.
(9) Forrest, J. A.; Dalnoki-Veress, K. *Adv. Colloid Interface Sci.* **2001**, *94* (1−3), 167−196.
(10) Keddie, J. L.; Jones, R. A. L.; Cory, R. A. *Europhysics Lett.* **1994**, *27* (1), 59−64.
(11) Torres, J. A.; Nealey, P. F.; de Pablo, J. J. *Phys. Rev. Lett.* **2000**, *85*, 3221−3224.
(12) Jiang, C. Y.; Markutsya, S.; Tsukruk, V. V. *Adv. Mater.* **2004**, *16* (2), 157.
(13) Decher, G. *Science* **1997**, *277* (5330), 1232−1237.
(14) Bertrand, P.; Jonas, A.; Laschewsky, A.; Legras, R. *Macromol. Rapid Commun.* **2000**, *21*, 319−348.
(15) Mamedov, A. A.; Kotov, N. A.; Prato, M.; Guldi, D. M.; Wicksted, J. P.; Hirsch, A. *Nat. Mater.* **2002**, *1*, 190−194.
(16) Dong, W. F.; Sukhorukov, G. B.; Mohwald, H. *Phys. Chem. Chem. Phys.* **2003**, *5*, 3003−3012.
(17) Dubreuil, F.; Shchukin, D. G.; Sukhorukov, G. B.; Fery, A. *Macromol. Rapid Commun.* **2004**, *25*, 1078−1081.
(18) Sukhorukov, G. B.; Shchukin, D. G.; Dong, W. F.; Mohwald, H.; Lulevich, V. V.; Vinogradova, O. I. *Macromol. Chem. Phys.* **2004**, *205*, 530−535.
(19) Shulha, C.; Markutsya, S.; Shulha, H.; Tsukruk, V. V. *Adv. Mater.* **2005**, *17*, 1669−1673.
(20) Dong, W. F.; Ferri, J. K.; Adalsteinsson, T.; Schonhoff, M.; Sukhorukov, G. B.; Mohwald, H. *Chem. Mater.* **2005**, *17*, 2603−2611.
(21) Ruths, J.; Essler, F.; Decher, G.; Riegler, H. *Langmuir* **2000**, *16*, 8871−8878.
(22) G. Loglio, P. P.; Miller, R.; Makievski, A. V.; Ravera, F.; Ferrari, M.; Liggieri, L. Novel Methods to Study Interfacial Layers. In *Studies in Interface Science*; Möbius, D., Miller, R., Eds.; Elsevier: Amsterdam, 2001; Vol. 11, p 439.
(23) Ferri, J. K.; Miller, R.; Makievski, A. V. *Colloids Surf. A: Physicochem. Eng. Asp.* **2005**, *261*, 39−48.
(24) Ferri, J. K.; Dong, W. F.; Miller, R. *J. Phys. Chem. B* **2005**, *109*, 14764−14768.
(25) Evans, E. A.; Skalak, R.; Hochmuth, R. M. *CRC Crit. Rev. Bioeng.* **1979**, *3* (3), 181−330.
(26) Carin, M.; Barthes-Biesel, D.; Edwards-Levy, F.; Postel, C.; Andrei, D. C. *Biotechnol. Bioeng.* **2003**, *82* (2), 207−212.
(27) Helm, C. A.; Laxhuber, L.; Losche, M.; Mohwald, H. *Colloid Polym. Sci.* **1986**, *264* (1), 46−55.
(28) Pieper, G.; Rehage, H.; Barthes-Biesel, D. *J. Colloid Interface Sci.* **1998**, *202* (2), 293−300.
(29) Lakes, R. *Adv. Mater.* **1993**, *5*, 293−296.
(30) Nolte, A. J.; Rubner, M. F.; Cohen, R. E. *Macromolecules* **2005**, *38*, 5367−5370.

MA0516485